Turbulence, Heat and Mass Transfer 10

Numerical Analysis of Parcel Tracking in Large Eddy Simulation of Polydispersed Multiphase Flows: Assessment of different Parcel Modeling Techniques

L. Bahramian, F.X. Trias, C. Oliet and C.D. Pérez-Segarra
Heat and Mass Transfer Technological Center, Technical University of Catalonia
Carrer de Colom 11, 08222 Terrassa (Barcelona), Spain; www.cttc.upc.edu
{linda.bahramian, francesc.xavier.trias, carles.oliet, cdavid.perez.segarra}@upc.edu

Abstract – In order to assess the impacts of parcel modeling, the Eulerian-Lagrangian method, by using the Particle-In-Cell model, is implemented for a three-dimensional polydispersed two-phase turbulent flow. First, the benchmark case of a confined jet presented by Hishida (1987) is used for validation. After determining a particle size distribution, the hybrid parcel model, which is a combination of two standard parcel models: the Number Fixed Model (NFM) and the Volume Fixed Model (VFM), has been designed based on the Sauter Mean Diameter (SMD). Later on, the velocity profiles of the dispersed phase were compared for these three parcel models. This comparison will allow us to study and assess the capacities and lacks regarding these parcel modeling techniques for design and optimization targets of different applications of dispersed multiphase flows. Results show that for the small particle sizes, the hybrid parcel model presents favorable agreement and fewer differences in the mean and the Root Mean Square (RMS) particle velocity profiles compared to the VFM, and in comparison to the NFM, this parcel model shows fewer discrepancies in particle velocity profiles for the large particle sizes.

1. Introduction

Numerical simulations of dispersed multiphase flows play an essential role in industrial applications such as combustion chambers, dispersion of pollutants, evaporative cooling, particle separators, etc. It can be applied both for analysis and design purposes. The Eulerian-Lagrangian approach is well-suited where thousands to millions of particles are present in the desired domain. The Eulerian part is used for the continuous phase, and the Lagrangian for the dispersed one.

Tracking millions of particles based on the Lagrangian approach through Large Eddy Simulation (LES) is computationally expensive. In order to decrease the computational cost, one approach is to track parcels instead of each individual particle. A parcel is a group of particles with similar characteristics, such as diameter and velocity, which move together through the continuous phase. To accomplish this assumption, parcel modeling should be analyzed in different aspects to achieve sufficient accuracy and particle dispersion.

Watanabe et al. (2015) studied two common types of arranging particles for parcels in a polydisperse configuration, the NFM and the VFM. The NFM presents the parcels with the same number of particles, while the VFM provides the parcels with the same volume and a distinguished number of particles. Based on the conclusions presented by Watanabe et al. (2015), the discrepancies generated by these two parcel models are acceptable where the number of

particles per parcel, N_p, is in O(10^0) while the parcels with N_p in O(10^1) significantly affect the results.

In order to enhance the computational cost versus accuracy, one way is to increase the N_p in some diameter ranges. Therefore, a hybrid model, which is a combination of these two models, was proposed by Bahramian et al. (2022) which is studied for the particle-laden turbulent flow benchmark case of Borée et al. (2001). The parcel arrangement is shown in Fig. 1. In this approach first, the SMD should be determined. The SMD in terms of number distributions of particle size classes is defined by Azzopardi (2011) as:

$$D_{pq} = \left[\frac{\sum_{i=1}^{\infty} n_i D_i^p}{\sum_{i=1}^{\infty} n_i D_i^q} \right]^{1/(p-q)} \tag{1}$$

where $p = 3$ and $q = 2$. n and D are the number distribution and the diameter of the particle sizes, respectively.

After determining the SMD, the particles with diameters below the SMD are arranged by the NFM, and the rest of them are arranged based on the VFM. As mentioned in the work of Watanabe et al. (2015), with increasing the N_p in the NFM, this approach showed some discrepancies in the particle classes with the larger diameters, and the VFM showed some disagreements in the particle classes with the small diameters. So the idea behind designing a combination model of these two models was to enhance the parcel class behaviors to reach an optimal solution.

2. Governing Equations

Here, the governing equations that have been used are summarized. The particle motion in a continuous phase applying a Lagrangian method can be defined by Newton's law. The primary contribution to this subject was made by Basset (1888), Boussinesq (1885) and Oseen (1927), called BBO-equation. Maxey and Riley (1983) carried out an extensive study of the BBO-equation in non-uniform flow for small rigid particles. Thus, the nth particle position and momentum are calculated as:

$$\frac{\mathrm{d}\mathbf{x_p^n}}{\mathrm{d}t} = \mathbf{v_p^n} \tag{2}$$

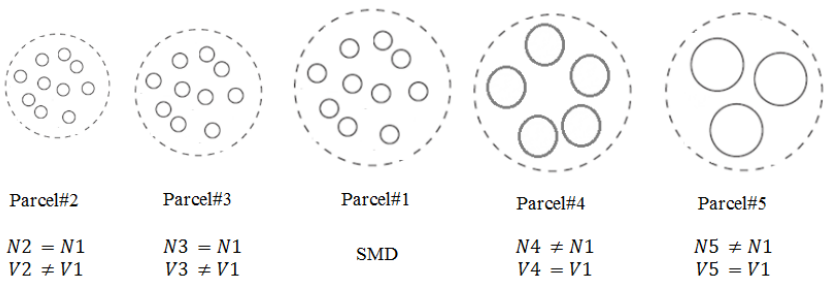

Figure 1: Schematic of the new parcel model Bahramian et al (2022).

$$m_{\mathrm{p}}^{n}\frac{\mathrm{d}\mathbf{v_p^n}}{\mathrm{d}t}=\sum_{i}\mathbf{F_i} \tag{3}$$

where $\mathbf{x_p^n}$, $\mathbf{v_p^n}$, and m_p^n are the nth particle center location, velocity, and mass. The sum of forces applied on the right-hand side of Eq. (3) consists of all the relevant forces acting over the particles, e.g., drag, gravity, added mass, pressure gradient force, etc. The assumption is made that the particles are large enough so Brownian or non-continuum motion of the particles may be negligible. Therefore Eq. (3) under the effect of drag and buoyancy forces can be formulated as:

$$m_{\mathrm{p}}^{n}\frac{\mathrm{d}\mathbf{v_p^n}}{\mathrm{d}t}=\frac{1}{2}\rho_{\mathrm{c}}C_D A_{\mathrm{p}}^{n}\left|\mathbf{u}(\mathbf{x_p^n})-\mathbf{v_p^n}(\mathbf{x_p^n})\right|\left(\mathbf{u}(\mathbf{x_p^n})-\mathbf{v_p^n}(\mathbf{x_p^n})\right)+\left(1-\frac{\rho_{\mathrm{c}}}{\rho_{\mathrm{p}}}\right)m_{\mathrm{p}}^{n}\mathbf{g} \tag{4}$$

where ρ_{c} and ρ_{p} are the fluid's density and the particle's density, C_D is the drag coefficient, A_{p}^{n}, the particle cross-section area, $\mathbf{g}$, gravitational acceleration vector and $\mathbf{u}(\mathbf{x_p^n})$ is the fluid's velocity at the nth particle's position.

The behavior of viscous incompressible continuous fluids is governed by the Navier-Stokes (NS) equations, which are studied in detail by Sagaut (2005). They are approximated by:

$$\nabla\cdot\ \mathbf{u}=0 \tag{5}$$

$$\rho_{\mathrm{c}}\left[\frac{\partial\mathbf{u}}{\partial t}+\nabla\cdot(\mathbf{uu})\right]=-\nabla p+\mu\nabla^2\mathbf{u}+\mathbf{S_u}\quad,\quad\mathbf{S_u}=-\sum_{n=1}^{N_{\mathrm{p}}}\frac{m_{\mathrm{p}}^{n}\mathbf{f_{cp}^n}}{V_{\mathrm{cell}}} \tag{6}$$

where p, μ, and $\mathbf{S_u}$ are the pressure, the dynamic viscosity, and the momentum source term, respectively, while $\mathbf{f_{cp}^n}$, V_{cell}, and N_p are the fluid-particle interaction force per unit mass of the particle, the volume of the computational cell, and the number of particles situated in a computational cell.

3. Results and Discussions

The benchmark case of Hishida (1987), which is shown in Fig. 2, is selected for validation purposes. It is a vertical descending jet loaded with particles in the center zone. The configuration consists of two concentric cylinders, an injector and a pipe, respectively, with diameters of 13 mm and 60 mm and a domain length of 300 mm. The flow is isothermal, incompressible and turbulent. The numerical simulations are carried out by an in-house parallel C++/MPI CFD code called TermoFluids which is implemented based on the finite volume method and symmetry-preserving discretization of the momentum equation (Trias et al. 2014).

3.1 Validation

To validate the numerical simulation, the heavy particle distribution from the benchmark case of Hishida (1987) is chosen, where the particles have diameters of 64.4 μm and a density of 2590 kg/m^3. The simulation involves tracking all individual particles without employing parcel modeling.

Fig. 3 and Fig. 4 show the radial profiles of the mean and RMS streamwise velocity of the carrier and dispersed phase at the different sections of the domain perpendicular to the direction of the flow. As can be seen, the numerical simulation is in good agreement with the

experimental data both for the continuous and dispersed phase.

3.2 Designing the hybrid parcel model

To investigate the different parcel models, a particle size distribution is established, where particles are categorized based on mean diameter classes of 20, 30, 40, 50, 60, 70, 80, 90, and 100 μm, with SMD of 60 μm. The first step for designing the hybrid parcel model is determining the N_p for the SMD. Therefore, for the particle classes with diameters above the SMD, we arrange the N_p by fixing the parcel volume equal to the one corresponding to the SMD (using the VFM), and for the particle classes with diameter below the SMD, we fix the N_p equal to the one corresponding to the SMD (using the NFM). As shown in the work of Watanabe et al. (2015), by increasing the N_p, the NFM has shown some discrepancies for the particle classes with diameters above the SMD. Thus, for determining the number of particles for the SMD, we have increased the N_p using the NFM to see where the discrepancies appear, especially for the particles with diameters above the SMD. The streamwise profiles of particle mean velocity at r=0 for the particle classes equal and above the SMD comparing the no-parcel model with the NFM are presented in Fig. 5 and Fig. 6. We have set the N_p to 5, 10, 20 and 40 in the NFM. As can be seen in Fig. 5, the particle classes of the SMD ($dp = 60\mu m$) have started showing some discrepancies from N_p above 20 and the particle classes with $dp = 70\mu m$ started to show disagreements for N_p equal 20. According to Fig. 6, particle classes with $dp = 80\mu m$ started to show some diversity for N_p equal to 10, and for particle classes with $dp = 90\mu m$, the discrepancies started for N_p equal to 5. In the hybrid parcel model, the particle classes with diameters above the SMD are arranged by the VFM, which signifies that the volume of parcels for these diameters will be equal to the one with the SMD. According to these figures, the N_p for these classes should not be in the zones where disagreements began. Therefore, according to these

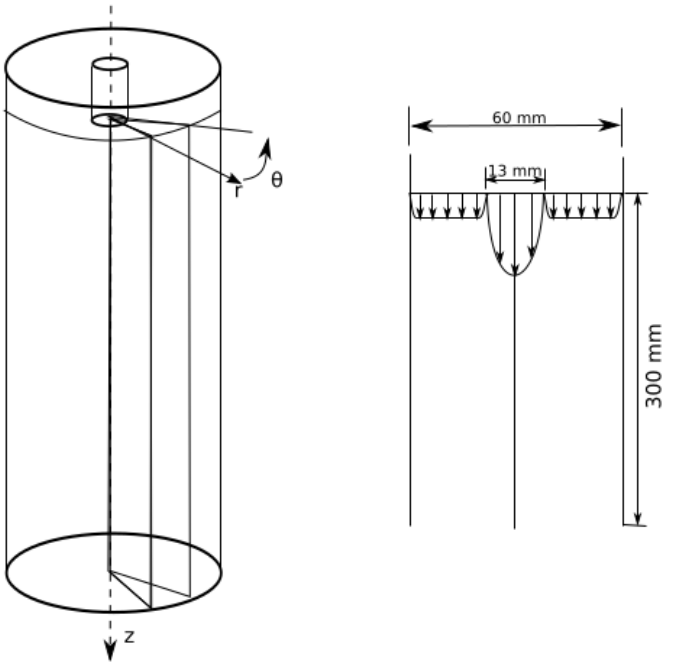

Figure 2: Sketch of the Hishida benchmark case.

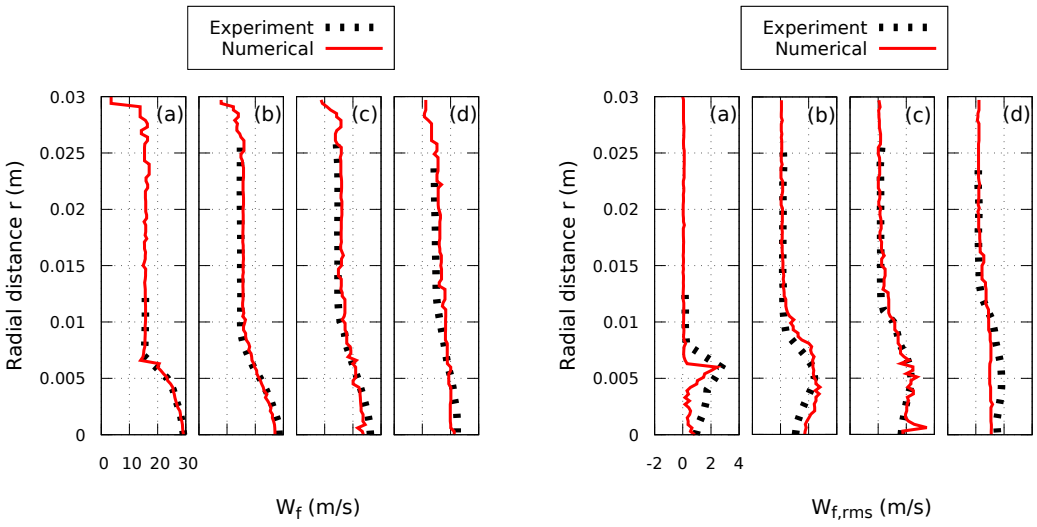

Figure 3: Radial profiles of fluid mean streamwise velocity (left) and fluid RMS streamwise velocity (right) for Hishida benchmark case. Circle: Experiment; solid line: Numerical simulation. (a) z=0m; (b) z=0.065m; (c) z=0.13m; (d) z=0.26m

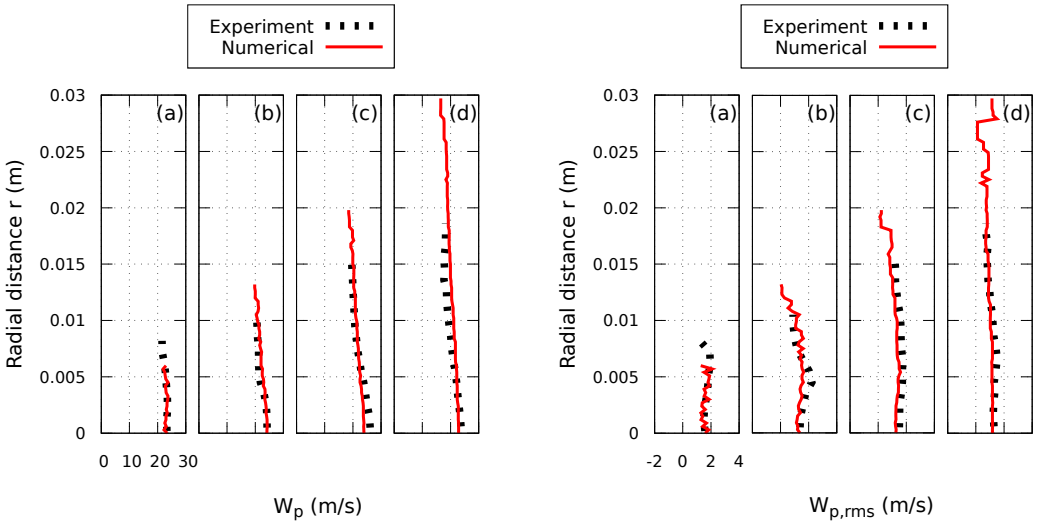

Figure 4: Radial profiles of particle mean streamwise velocity (left) and particle RMS streamwise velocity (right) for Hishida Benchmark case. Circle: Experiment; solid line: Numerical simulation. (a) z=0m; (b) z=0.065m; (c) z=0.13m; (d) z=0.26m

comparisons, the N_p for the SMD has been set to 15.

3.3 Comparing different parcel models

This section studies a comparison between the proposed hybrid model, the NFM, and the VFM. As the N_p has been set to 15 for the SMD of the hybrid model, the N_p is set to 15 for the NFM and for the VFM, the volume of parcels are fixed to the parcel of the SMD with $N_p = 15$. The streamwise profiles of particle mean and RMS velocity at the center-line for two different

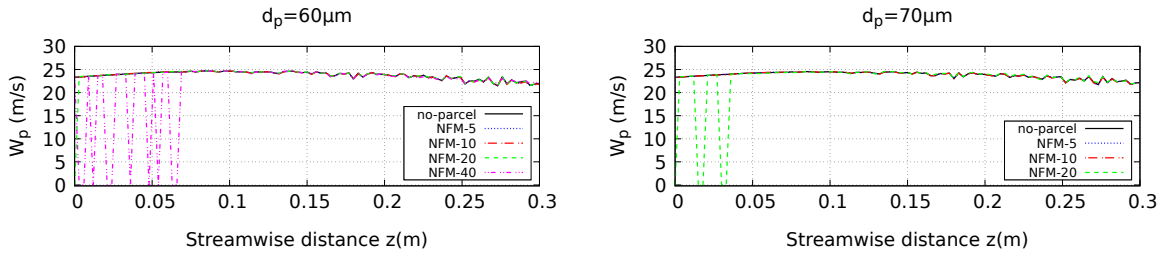

Figure 5: Streamwise profiles of particle mean velocity ($dp = 60\mu m$ and $dp = 70\mu m$) for the Hishida configuration comparing no-parcel and the NFM model (the number in NFM presents N_p).

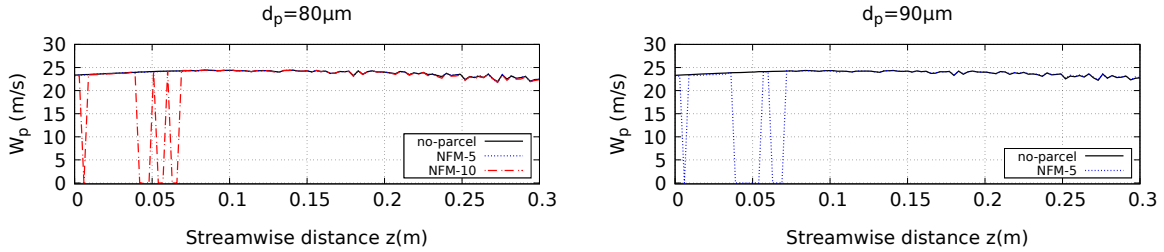

Figure 6: Streamwise profiles of particle mean velocity ($dp = 80\mu m$ and $dp = 90\mu m$) for the Hishida configuration comparing no-parcel and the NFM model(the number in NFM presents N_p).

particle diameters are shown in Fig. 7 and Fig. 8. The objective of this comparison was to see whether the hybrid model could present better behavior compared to the VFM for particles with diameters smaller than the SMD and to show fewer discrepancies compared to the NFM for particles with diameters above the SMD. As can be observe in Fig. 7, for particle diameters of $dp = 20\mu m$, the behavior of the hybrid model is in good agreement with the no-parcel model, while the VFM presents some deviations in both the mean and the RMS velocity profiles. The presence of zero velocities indicates the absence of parcels in those specific positions, leading to inadequate dispersion for particle classes of small diameters. This discrepancy is particularly notable at the initial section of the streamwise direction along the center line. Fig. 8 for particle diameters of $dp = 80\mu m$ shows that the hybrid model accurately aligns with the no-parcel model's values for both the mean and the RMS velocity profiles. However, the NFM presents some discrepancies and includes instances of zero velocities at the beginning of the domain. This observation implies the absence of parcels with particle diameters of 80 μm at the initial section of the streamwise direction along the center line, indicating inadequate dispersion for larger particles.

4. Conclusions

The focus of the present investigation is on the implementation of an innovative strategy for parcel modeling. This is accomplished by integrating the NFM and the VFM based on the SMD.

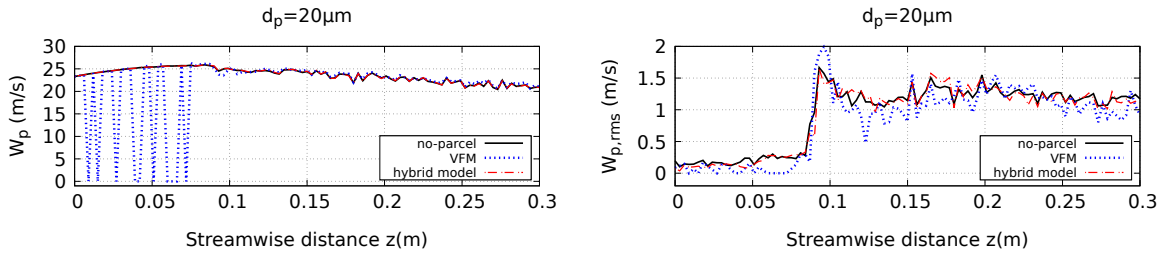

Figure 7: Streamwise profiles of particle mean and RMS velocity ($dp = 20\mu m$) for the Hishida configuration comparing no-parcel, VFM and hybrid model.

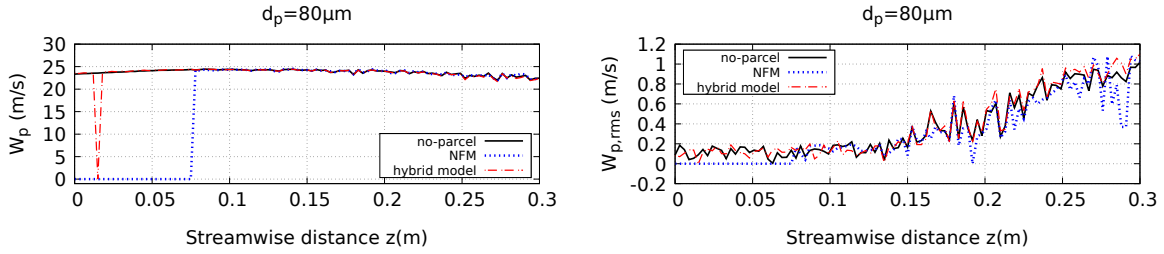

Figure 8: Streamwise profiles of particle mean and RMS velocity ($dp = 80\mu m$) for the Hishida configuration comparing no-parcel, NFM and hybrid model.

The numerical results for the velocity profiles of both fluid and particles in the radial direction of different sections track the experimental data properly. The N_p in the hybrid parcel model is arranged based on the SMD, using the VFM for particle diameters above the SMD and the NFM for the particle diameters smaller than the SMD. Compared to the VFM, the hybrid model enhanced parcel dispersion and reduced disparities within the dispersed phase's mean and RMS velocity profiles for particle diameters smaller than the SMD. Considering the NFM results, the hybrid model showed improved conformity and diminished discrepancies in the mean and the RMS velocity profiles for parcels with particle diameters above the SMD. In summary, the preliminary results showed that the proposed hybrid parcel model presented an appropriate degree of precision and particle dispersion compared to the no-parcel model. Further investigation regarding the quantitative values of the computational costs, particle dispersion and particle volume fraction comparing these three parcel models will be carried out.

Acknowledgements

This work has been developed within the EU H2020 Clean Sky 2 research project "A New proTection devIce for FOD - ANTIFOD" (grant agreement Nº 821352).

Linda Bahramian acknowledges the financial support from the Secretariat of Universities and Research of the Generalitat de Catalunya and the European Social Fund, FI AGAUR Grant (2019 FI_B 01205) and the UPC-Santander Grant. Carles Oliet, as a Serra Húnter associate professor, acknowledges the Catalan Government for the support through this Programme.

References

1. K. Hishida. Turbulence characteristics of gas-solids two-phase confined jet (effect of particle density). *Japanese Journal of Multiphase Flow*, 1(1):56-69, 1987.
2. H. Watanabe, D. Uesugi, M. Muto. Effects of parcel modeling on particle dispersion and interphase transfers in a turbulent mixing layer. *Advanced Powder Technology*, 26(6):1719-1728, 2015.
3. L. Bahramian, J. Muela, C. Oliet, C.D. Pérez-Segarra, F.X. Trias. An Efficient Strategy of Parcel Modeling for Polydispersed Multiphase Turbulent Flows. *World Congress in Computational Mechanics and ECCOMAS Congress*, 2022.
4. J. Borée, T. Ishima and T. Flour, The effect of mass loading and inter-particle collisions on the development of the polydispersed two-phase flow downstream of a confined bluff body *Journal of Fluid Mechanics*, 443:129-165, 2001.
5. Azzopardi, B.J., Sauter mean diameter. *Thermopedia, [Online]. Available: http://www.thermopedia.com/content/1108/. [Accessed 01 03 2013]*, 2011.
6. Basset, A.B., On the motion of a sphere in a viscous liquid. *Philosophical Transactions of the Royal Society of London A: Mathematical, Physical and Engineering Sciences*, 179:43-63, 1888.
7. Boussinesq, J., Sur la resistance qu'oppose un fluide indefini en repos, sans pesanteur, au mouvement varie d'une sphere solide qu'il mouille sur toute sa surface, quand les vitesses restent bien continues et assez faibles pour que leurs carres et produits soient negligiables. *CR Acad. Sc. Paris*, 100:935-937, 1885.
8. Oseen, C.W., Hydrodynamik. *Akademische Verlagsgesellschaft*,1927.
9. Maxey, M.R. and Riley, J.J., Equation of motion for a small rigid sphere in a nonuniform flow. *The Physics of Fluids*, 26(4):883-889, 1983.
10. Sagaut, P., Large eddy simulation for incompressible flows: an introduction. *Springer Science & Business Media*, 2005.
11. S.L. TermoFluids. *http://www.termofluids.com/*.
12. F.X. Trias, O. Lehmkuhl, A. Oliva, C.D. Pérez-Segarra, R.W.C.P. Verstappen. Symmetry-preserving discretization of Navier–Stokes equations on collocated unstructured grids. *Journal of Computational Physics*, 258(1):246-267, 2014.